

- (15) G. J. Kubas, submitted for publication in *Inorg. Chem.*
 (16) D. C. Moody and R. R. Ryan, *J. Chem. Soc., Chem. Commun.*, 503 (1976).
 (17) D. C. Moody and R. R. Ryan, *Inorg. Chem.*, **16**, 2473 (1977).
 (18) P. G. Linert, *J. Appl. Crystallogr.*, **8**, 568 (1975).
 (19) (a) J. de Meulenaer and H. Tompa, *Acta Crystallogr.*, **19**, 1014 (1965);
 (b) L. K. Templeton and D. H. Templeton, Abstracts, American

- Crystallographic Association Summer Meeting, Storrs, Conn., June 1973, No. E10.
 (20) S. J. La Placa and J. A. Ibers, *Inorg. Chem.*, **5**, 405 (1966).
 (21) K. W. Muir and J. A. Ibers, *Inorg. Chem.*, **8**, 1921 (1969).
 (22) D. C. Moody and R. R. Ryan, *Inorg. Chem.*, **15**, 1823 (1976).
 (23) P. G. Eller, R. R. Ryan, and D. C. Moody, *Inorg. Chem.*, **15**, 2442 (1976).
 (24) G. J. Kubas and R. R. Ryan, *Cryst. Struct. Commun.*, **6**, 295 (1977).

Contribution from the Department of Chemistry, University of North Carolina, Chapel Hill, North Carolina 27514

Structure and Properties of Pseudotetrahedral Dichloro(2-(2-dimethylaminoethyl)pyridine)copper(II)

ROXY B. WILSON, JOHN R. WASSON, WILLIAM E. HATFIELD, and DEREK J. HODGSON*

Received June 28, 1977

The complex dichloro(2-(2-dimethylaminoethyl)pyridine)copper(II), $\text{Cu}(\text{C}_9\text{H}_{14}\text{N}_2)_2\text{Cl}_2$ or $\text{Cu}(\text{DMAEP})\text{Cl}_2$, has been synthesized and its crystal and molecular structure has been determined from three-dimensional counter x-ray data. The complex crystallizes in the triclinic space group $P\bar{1}$ with two formula units in a cell of dimensions $a = 7.348$ (3) Å, $b = 8.875$ (4) Å, $c = 9.982$ (4) Å, $\alpha = 74.69$ (2)°, $\beta = 99.06$ (2)°, and $\gamma = 109.65$ (2)°. The observed and calculated densities are 1.59 and 1.603 g cm⁻³. The structure was refined by full-matrix least-squares methods to an *R* factor (on *F*) of 0.031 using 2084 independent intensities. The structure consists of discrete monomeric $\text{Cu}(\text{DMAEP})\text{Cl}_2$ units with four-coordinate pseudotetrahedral geometry at the copper(II) centers. The copper-ligand bond lengths are normal, but the six-membered chelate ring adopts the half-chair conformation rather than the boat conformation observed in a number of analogues. Electron paramagnetic resonance and electronic spectral data for $\text{Cu}(\text{DMAEP})\text{Cl}_2$ and its isomorphous bromo analogue afford significant support for spectral-structure correlations; these DMAEP complexes exhibit novel single-line EPR solution spectra at room temperature.

Introduction

Complexes of the type $\text{Cu}(\text{AEP})\text{X}_2$, where AEP is 2-(2-aminoethyl)pyridine and X is a halogen, were first synthesized by Uhlig and Maaser¹ who suggested that these compounds would be discrete dihalogen bridged dimers with square-pyramidal geometry about the copper ions. However, when X is chlorine² or bromine,³ the compounds are best described as six-coordinate polymers consisting of monohalogen bridged chains connected by dihalogen bridges, the geometry about copper being severely distorted octahedral. Since there are two available pathways for superexchange, the magnetic properties⁴ are difficult to account for accurately.

The copper(II) ion has a six-coordinate geometry in polymeric $\text{Cu}(\text{py})_2\text{X}_2$ compounds.⁵⁻⁷ When pyridine is replaced by 2-methylpyridine, the methyl groups sterically block coordination at the sixth binding site on copper and $\text{Cu}(\text{2-Me-py})_2\text{X}_2$ compounds are five-coordinate dimers.^{8,9} In order to assess the effects of alkyl substitution on AEP in complexes of the general type CuLX_2 , we examined 2-(2-methylaminoethyl)pyridine (MAEP) compounds. A tightly bound monochloro-bridged chain structure with tetragonal-pyramidal geometry about the copper ion was found¹⁰ for $\text{Cu}(\text{MAEP})\text{Cl}_2$. When X = Br, the complex is a dibromo-bridged dimer with trigonal-bipyramidal geometry at copper.¹¹ In both examples coordination was apparently blocked at the sixth site on the copper centers by a proton on C(4) of the six-membered chelate ring rather than by the presence of the methyl group.

Complexes of the types CuLX_2 (L = bidentate ligand) and CuA_2X_2 (A = monodentate ligand) adopt a wide variety of structures.^{2,3,5-9,12-18} $\text{Cu}(\text{MAEP})\text{Cl}_2$ is only the second of its type, and $\text{Cu}(\text{MAEP})\text{Br}_2$ is the first example of a trigonal-bipyramidal, bromine-bridged dimer. In view of the unusual structural and magnetic properties of copper complexes with AEP and substituted AEP ligands and the observation that one methyl substituent does not dominate the stereochemistry of the complexes, we have undertaken a structural and

spectroscopic study of the disubstituted complex $\text{Cu}(\text{DMAEP})\text{Cl}_2$ (DMAEP = 2-(2-dimethylaminoethyl)pyridine).

Experimental Section

Bright green $\text{Cu}(\text{DMAEP})\text{Cl}_2$ was prepared by addition of 0.361 g (0.002 mol) of copper(II) chloride dihydrate to a solution containing 0.330 g (0.002 mol) of DMAEP in 40 mL of absolute methanol. The resultant green solution was stirred and refrigerated; crystals formed after a few days. Brown $\text{Cu}(\text{DMAEP})\text{Br}_2$ was prepared similarly using copper(II) bromide. The copper content of the complexes was determined by EDTA titrations.

Weissenberg and precession photography indicated that $\text{Cu}(\text{DMAEP})\text{Cl}_2$ crystals belonged to the triclinic system, the space group being either C_1^1-P1 or $C_1^1-P\bar{1}$. The centrosymmetric space group was chosen and successful refinement of the structure demonstrated that this choice was correct. Observations were made at 22° using $\text{Mo K}\alpha_1$ radiation with an assumed wavelength of 0.7093 Å. The cell constants, obtained by least-squares methods, are $a = 7.348$ (3) Å, $b = 8.875$ (4) Å, $c = 9.982$ (4) Å, $\alpha = 74.69$ (2)°, $\beta = 99.06$ (2)°, and $\gamma = 109.65$ (2)°. The observed density of 1.59 g cm⁻³, obtained by flotation in a mixture of bromoform and benzene, is in good agreement with the calculated density of 1.603 g cm⁻³ assuming two monomeric units in the cell.

The crystal used to collect diffraction data was a thin plate with faces (100), ($\bar{1}00$), (010), (0 $\bar{1}0$), (011), and (0 $\bar{1}1$) and was mounted roughly perpendicular to the (100) face. The separations between opposite pairs of faces were as follows: (100) and ($\bar{1}00$), 0.058 cm; (010) and (0 $\bar{1}0$), 0.005 cm; (011) and (0 $\bar{1}1$), 0.020 cm. Intensity data were collected on a Picker four-circle automatic diffractometer equipped with a graphite monochromator using $\text{Mo K}\alpha$ radiation at a takeoff angle of 1.2°. Data were collected in the θ - 2θ scan mode from 0.65° below the calculated $\text{Mo K}\alpha_1$ position to 0.65° above the calculated $\text{Mo K}\alpha_2$ position at the rate of 1°/min with 10-s stationary-counter stationary-crystal background counts at both ends of the scan. The pulse height analyzer was set for an approximately 90% window centered on the $\text{Mo K}\alpha$ peak.

An independent set of data ($h, \pm k, \pm l$) was collected with a maximum value for 2θ of 55° ($\text{Mo K}\alpha$), beyond which there were few intensities greater than background. The three standard reflections which were recorded at intervals of 100 reflections showed no sys-

Table I. Fractional Coordinates for [Cu(DMAEP)Cl₂] with Standard Deviations in Parentheses

Atoms	x	y	z
Cu	0.0904 (1)	-0.2347 (1)	0.2420 (1)
Cl(1)	0.2634 (1)	-0.3249 (1)	0.4335 (1)
Cl(2)	0.2298 (1)	-0.2593 (1)	0.0699 (1)
N(1)	0.0726 (3)	-0.0394 (3)	0.2984 (2)
N(2)	-0.1856 (3)	-0.3059 (3)	0.1665 (2)
C(2)	-0.0871 (4)	0.0031 (3)	0.2952 (3)
C(3)	-0.0733 (5)	0.1515 (4)	0.3251 (3)
C(4)	0.1030 (6)	0.2563 (4)	0.3565 (4)
C(5)	0.2664 (5)	0.2115 (4)	0.3603 (3)
C(6)	0.2467 (4)	0.0636 (4)	0.3327 (3)
C(7)	-0.2824 (4)	-0.1067 (4)	0.2577 (4)
C(8)	-0.3031 (4)	-0.2833 (4)	0.2637 (3)
C(9)	-0.2352 (6)	-0.4848 (4)	0.1761 (4)
C(10)	-0.2247 (5)	-0.2228 (5)	0.0219 (3)
H(3)	-0.181 (6)	0.179 (5)	0.321 (4)
H(4)	0.089 (5)	0.351 (5)	0.374 (4)
H(5)	0.382 (5)	0.271 (4)	0.386 (4)
H(6)	0.372 (5)	0.020 (4)	0.343 (4)
H(7)	-0.371 (6)	-0.108 (5)	0.314 (4)
H(7)'	-0.334 (5)	-0.059 (4)	0.172 (4)
H(8)	-0.263 (4)	-0.340 (3)	0.354 (3)
H(8)'	-0.439 (4)	-0.339 (4)	0.243 (3)
H(9)	-0.158 (5)	-0.509 (4)	0.119 (4)
H(9)'	-0.198 (5)	-0.532 (5)	0.278 (4)
H(9)''	-0.354 (7)	-0.524 (5)	0.142 (5)
H(10)	-0.178 (5)	-0.114 (5)	0.013 (3)
H(10)'	-0.166 (5)	-0.255 (4)	-0.037 (4)
H(10)''	-0.354 (6)	-0.254 (5)	-0.009 (4)

tematic decline as a function of exposure time. The data were processed using the formula of Ibers and co-workers¹⁹ for the estimated standard deviation $\sigma(I) = [C + 0.25(t_s/t_b)^2(B_H + B_L) + p^2I^2]^{1/2}$; the value of p was assigned as 0.045.²⁰ The values of I and $\sigma(I)$ were corrected for absorption and for Lorentz-polarization effects using the expression²¹

$$\frac{1}{Lp} = \frac{2 \sin 2\theta}{\cos^2 2\theta_m + \cos^2 2\theta}$$

where θ_m , the angle of the monochromator, was 12.0°. The attenuation coefficient for Cu(DMAEP)Cl₂ using Mo K α radiation was 22.17 cm⁻¹ and the transmission coefficients ranged from 0.99 to 0.52. Of the 2758 nonzero data collected, 2084 had intensities greater than three times their estimated standard deviation.

Electronic spectra were obtained with a Cary Model 17 recording spectrophotometer using matched 1.0-cm cells. Mull (transmission) electronic spectra were taken using a method described previously.²² Electron paramagnetic resonance (EPR) spectra were recorded on

a Varian E-3 X-band spectrometer. Quartz sample tubes were employed for polycrystalline samples and frozen solutions. Spectra were calibrated using diphenylpicrylhydrazyl (DPPH, $g = 2.0036$) as a field marker and a solution of oxobis(2,4-pentanedionato)vanadium(IV) in benzene²³ as a field marker and field sweep monitor.

Solution and Refinement of the Crystal Structure

Examination of a three-dimensional Patterson function yielded the positions of copper and both chlorine atoms, and two cycles of least-squares refinement were carried out on these positions. All least-squares refinements in this study were carried out on F , the function minimized being $\sum w(|F_o| - |F_c|)^2$ where the weight, w , is taken as $4F_o^2/\sigma^2(F_o^2)$. When calculating F_c , the atomic scattering factors for nonhydrogen atoms were taken from ref 24a and those for H from Stewart, Davidson, and Simpson.²⁵ The effects of anomalous dispersion of Cu and Cl were also included in the calculation of F_c ; the values of $\Delta f'$ and $\Delta f''$ again were taken from ref 24b. The remaining nonhydrogen atoms were located from a difference Fourier synthesis, and isotropic least-squares refinement of these positions yielded values of the conventional residuals $R_1 = 0.104$ and $R_2 = 0.137$, where $R_1 = \sum(|F_o| - |F_c|)/\sum|F_o|$ and $R_2 = [\sum w(|F_o| - |F_c|)^2/w(F_o^2)^{1/2}]^{1/2}$; anisotropic refinement of these atoms led to $R_1 = 0.046$ and $R_2 = 0.071$. The subsequent difference Fourier synthesis revealed the positions of all 14 hydrogen atoms. Isotropic refinement of these positions along with anisotropic refinement of the nonhydrogen atoms led to final values of $R_1 = 0.031$ and $R_2 = 0.041$. No correction for secondary extinction was necessary.

In the final cycle of least-squares refinement, no atom parameter shifted by more than 0.60 times its estimated standard deviation, indicating that refinement had converged. The value of R_2 showed no unusual dependence on $|F|$ or $\sin \theta$, indicating that our weighting scheme was appropriate. In the final difference Fourier synthesis there was no peak higher than 0.58 e Å⁻³, the value for an average hydrogen atom being 0.7 e Å⁻³. The positional and thermal parameters for Cu(DMAEP)Cl₂ are listed in Tables I and II; observed and calculated structure amplitudes are available.²⁶

Results and Discussion

Description of the Structure of Cu(DMAEP)Cl₂. The structure consists of discrete monomeric Cu(DMAEP)Cl₂ units as shown in Figure 1. The geometry about each copper atom is four-coordinate pseudotetrahedral. The L₁-Cu-L₂ (where L₁ and L₂ are any two ligating atoms) angles are intermediate between the expected values for tetrahedral (109.5°) and square-planar geometries (90 or 180°), respectively. The average value of the six angles subtended at copper is 110.5°, which is much closer to the expected value for tetrahedral geometry (109.5°) than that for square-planar geometry (120°). As would be expected in either idealized geometry,

Table II. Thermal Parameters (U_{ij} in Å²) for [Cu(DMAEP)Cl₂]

Atom	U_{11}^a (or B)	U_{22}	U_{33}	U_{12}	U_{13}	U_{23}
Cu	0.0259 (2)	0.0396 (2)	0.0345 (2)	0.0149 (1)	-0.0026 (1)	-0.0138 (1)
Cl(1)	0.0360 (4)	0.0481 (4)	0.0384 (4)	0.0185 (3)	-0.0049 (3)	-0.0063 (3)
Cl(2)	0.0451 (5)	0.0881 (7)	0.0479 (4)	0.0331 (4)	0.0011 (3)	-0.0294 (4)
N(1)	0.0262 (11)	0.0325 (12)	0.0324 (11)	0.0091 (9)	-0.0000 (9)	-0.0098 (9)
N(2)	0.0271 (11)	0.0306 (12)	0.0287 (11)	0.0087 (9)	0.0003 (9)	-0.0059 (9)
C(2)	0.0357 (15)	0.0329 (14)	0.0297 (13)	0.0136 (12)	0.0030 (11)	-0.0051 (11)
C(3)	0.0485 (19)	0.0405 (17)	0.0544 (19)	0.0236 (15)	0.0004 (15)	-0.0156 (14)
C(4)	0.0743 (25)	0.0370 (18)	0.0514 (20)	0.0215 (17)	-0.0077 (17)	-0.0172 (15)
C(5)	0.0462 (19)	0.0421 (18)	0.0412 (17)	0.0003 (15)	-0.0045 (14)	-0.0143 (14)
C(6)	0.0333 (15)	0.0412 (16)	0.0403 (15)	0.0067 (13)	-0.0006 (12)	-0.0113 (13)
C(7)	0.0304 (15)	0.0424 (17)	0.0505 (18)	0.0170 (13)	0.0017 (13)	-0.0125 (14)
C(8)	0.0239 (14)	0.0375 (16)	0.0352 (15)	0.0064 (12)	0.0049 (11)	-0.0066 (12)
C(9)	0.0515 (21)	0.0365 (17)	0.0593 (22)	0.0077 (16)	0.0049 (18)	-0.0197 (16)
C(10)	0.0383 (19)	0.0644 (25)	0.0316 (16)	0.0154 (18)	-0.0008 (13)	-0.0049 (16)
Atom	$U, \text{Å}^2$	Atom	$U, \text{Å}^2$	Atom	$U, \text{Å}^2$	
H(3)	0.070 (12)	H(7)'	0.043 (9)	H(9)''	0.083 (14)	
H(4)	0.069 (12)	H(8)	0.031 (7)	H(10)	0.046 (10)	
H(5)	0.061 (11)	H(8)'	0.034 (8)	H(10)'	0.050 (9)	
H(6)	0.059 (10)	H(9)	0.056 (10)	H(10)''	0.069 (12)	
H(7)	0.064 (11)	H(9)'	0.069 (12)			

^a The form of the anisotropic thermal ellipsoid is $\exp[-2\pi^2(U_{11}h^2a^* + U_{22}k^2b^{*2} + U_{33}l^2c^* + 2U_{12}hka^*b^* + 2U_{13}hla^*c^* + 2U_{23}klb^*c^*)]$.

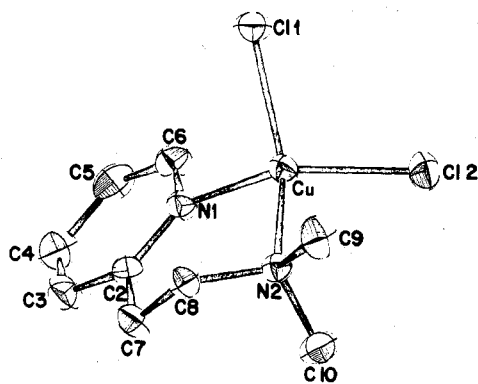


Figure 1. The coordination geometry of one molecule of $\text{Cu}(\text{DMAEP})\text{Cl}_2$.

Table III. Interatomic Distances in $[\text{Cu}(\text{DMAEP})\text{Cl}_2]$ (Å)

Cu-Cu	5.792 (2)	N(2)-C(10)	1.470 (4)
Cu-Cl(1)	2.241 (1)	C(3)-H(3)	0.90 (4)
Cu-Cl(2)	2.225 (1)	C(4)-H(4)	0.94 (4)
Cu-N(1)	2.007 (3)	C(5)-H(5)	0.88 (4)
Cu-N(2)	1.998 (2)	C(6)-H(6)	1.09 (4)
N(1)-C(2)	1.342 (4)	C(7)-H(7)	0.92 (4)
C(2)-C(3)	1.394 (4)	C(7)-H(7')	0.93 (3)
C(3)-C(4)	1.363 (5)	C(8)-H(8)	0.97 (3)
C(4)-C(5)	1.378 (5)	C(8)-H(8')	0.97 (3)
C(5)-C(6)	1.368 (5)	C(9)-H(9)	0.97 (4)
C(6)-N(1)	1.353 (4)	C(9)-H(9')	1.02 (4)
C(2)-C(7)	1.494 (4)	C(9)-H(9'')	0.88 (5)
C(7)-C(8)	1.509 (4)	C(10)-H(10)	0.89 (4)
N(2)-C(8)	1.486 (4)	C(10)-H(10')	0.93 (4)
N(2)-C(9)	1.485 (4)	C(10)-H(10'')	0.92 (4)

Table IV. Interatomic Angles in $[\text{Cu}(\text{DMAEP})\text{Cl}_2]$ (deg)

Cl(1)-Cu-Cl(2)	103.33 (4)	C(5)-C(6)-N(1)	122.4 (3)
Cl(1)-Cu-N(1)	97.32 (7)	C(6)-N(1)-C(2)	118.8 (3)
Cl(1)-Cu-N(2)	135.42 (7)	C(3)-C(2)-C(7)	118.8 (3)
Cl(2)-Cu-N(1)	132.72 (7)	N(1)-C(2)-C(7)	120.7 (2)
Cl(2)-Cu-N(2)	98.70 (7)	C(2)-C(7)-C(8)	118.0 (2)
N(1)-Cu-N(2)	95.34 (9)	C(7)-C(8)-N(2)	114.7 (2)
Cu-N(1)-C(2)	127.4 (2)	C(8)-N(2)-C(9)	107.9 (2)
Cu-N(1)-C(6)	113.7 (2)	C(8)-N(2)-C(10)	111.8 (2)
N(1)-C(2)-C(3)	120.5 (3)	C(9)-N(2)-C(10)	109.3 (3)
C(2)-C(3)-C(4)	120.4 (3)	Cu-N(2)-C(10)	115.1 (2)
C(3)-C(4)-C(5)	118.8 (3)	Cu-N(2)-C(9)	105.6 (2)
C(4)-C(5)-C(6)	119.1 (3)	Cu-N(2)-C(8)	106.7 (2)

atoms L_3 and L_4 are nearly equidistant from the plane determined by Cu, L_1 , and L_2 . The description of the complex as pseudotetrahedral rather than distorted square planar is in accord with the spectroscopic data (vide infra).

The interatomic distances, angles, and planes of interest in $\text{Cu}(\text{DMAEP})\text{Cl}_2$ are shown in Tables III-V. The two independent Cu-Cl distances of 2.225 (1) and 2.241 (1) Å are typical for terminal Cu-Cl bonds. There are no pertinent long range interactions. The shortest intermolecular separations are Cu-Cu, 5.792 (2) Å, Cl-Cl, 4.214 (2) Å, and Cu-Cl, 4.654 (2) Å, all of which are much greater than the sum of the van der Waals radii of the two atoms involved. The Cu-N(1) and Cu-N(2) distances of 2.007 (3) and 1.998 (2) Å are significantly shorter than those in $\text{Cu}(\text{MAEP})\text{Cl}_2^{10}$ and $\text{Cu}(\text{MAEP})\text{Br}_2^{11}$ owing to the relief of steric strain in the pseudotetrahedral configuration. Unlike $\text{Cu}(\text{MAEP})\text{Br}_2^{11}$ and $\text{Cu}(\text{MAEP})\text{Cl}_2^{10}$ where the methyl substituents seemed to have little, if any, steric effect on the geometry of the complex, the two methyl groups in $\text{Cu}(\text{DMAEP})\text{Cl}_2$ appear to block approach to one or both vacant coordination sites at the copper center. In a distorted tetrahedron the exact location of these two sites is difficult to determine, but it can be seen from Figure 1 that C(9) is blocking approach to the trigonal face of the tetrahedron determined by Cl(1), Cl(2), and N(2), while

Table V. Least-Squares Planes in $[\text{Cu}(\text{DMAEP})\text{Cl}_2]$

Plane	Atoms in plane	Distance ^a	Other atoms	Distance ^a
1	N(1)	-0.219	Cu	-0.580
	N(2)	0.197	C(7)	0.455
	C(2)	0.250		
	C(8)	-0.228		
2	Cu	0.009	N(2)	0.349
	N(1)	-0.023	C(8)	-0.487
	C(2)	0.025		
	C(7)	-0.011		
3	N(1)	0.008		
	C(2)	0.001		
	C(3)	-0.008		
	C(4)	0.005		
	C(5)	0.004		
	C(6)	-0.011		
4	Cu	0.0	N(1)	1.354
	Cl(1)	0.0	N(2)	-1.244
	Cl(2)	0.0		
5	Cu	0.0	Cl(2)	1.472
	Cl(1)	0.0	N(2)	-1.352
	N(1)	0.0		
6	Cu	0.0	Cl(1)	-1.373
	Cl(2)	0.0	N(1)	1.420
	N(2)	0.0		
7	Cu	0.0	Cl(2)	1.920
	Cl(1)	0.0	N(1)	-1.920
	N(2)	0.0		
8	Cu	0.0	Cl(1)	-2.001
	Cl(2)	0.0	N(2)	1.902
	N(1)	0.0		
9	Cu	0.0	Cl(1)	-1.511
	N(1)	0.0	Cl(2)	1.563
	N(2)	0.0		
10	Cl(1)	-0.668	Cu	-0.026
	Cl(2)	0.655		
	N(1)	0.941		
	N(2)	-0.929		

^a Distance out of calculated plane in Å.

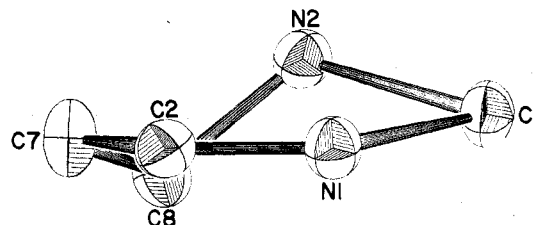


Figure 2. A view of the half-chair conformation adopted by the six-membered chelate ring in $\text{Cu}(\text{DMAEP})\text{Cl}_2$.

C(10) is blocking approach to the "bottom" face determined by N(1), N(2), and Cl(2).

The carbon-carbon distances and angles within the DMAEP moiety are normal for ligands of this type. In all other complexes of $\text{AEP}^{2,3,27,28}$ and substituted $\text{AEP}^{10,11,29-34}$ the six-membered chelate ring formed by Cu, N(1), C(2), C(7), C(8), and N(2) adopts the rigid boat conformation with N(1), N(2), C(2), and C(8) forming the base of the boat and Cu and C(7) lying above or below the plane formed by these four atoms. Whether Cu or C(7) is further from the plane is determined by the chelate bite, the N(1)-Cu-N(2) angle.¹¹ In $\text{Cu}(\text{DMAEP})\text{Cl}_2$, however, the four atoms which define the "base" of the boat are between 0.197 and 0.250 Å away from the least-squares plane calculated from their positions; the chelate ring is obviously not in the rigid boat conformation. Alternatively, if one calculates a plane through the four adjacent atoms Cu, N(1), C(2), and C(7), none of the four atoms deviates from this plane by more than 0.025 Å, with C(8) and N(2) 0.487 and 0.349 Å above and below the plane. This atomic arrangement describes a half-chair conformation (Figure 2) similar to the one adopted by cyclohexene. The

Table VI. Electronic Spectral Data

Compound	Solvent	$\lambda, \text{\AA}$	$\sigma, \text{M}^{-1} \text{cm}^{-1}$
Cu(DMAEP)Cl ₂	Dichloromethane	825 (133), 1050 (132)	
	Nujol	800, 1030, 400	
Cu(DMAEP)Br ₂	Dichloromethane	860 (252), 1080 (247)	
	Nujol	840, 1100, 430, 495	
Cu(biq)Cl ₂ ^b	Nujol	813, 901, 990	
Cu(biq)Br ₂	Nujol	893, 1000, 1075	

^a Molar absorptivity σ ($\text{M}^{-1} \text{cm}^{-1}$) in parentheses. ^b biq = 2,2'-biquinoline.⁴¹

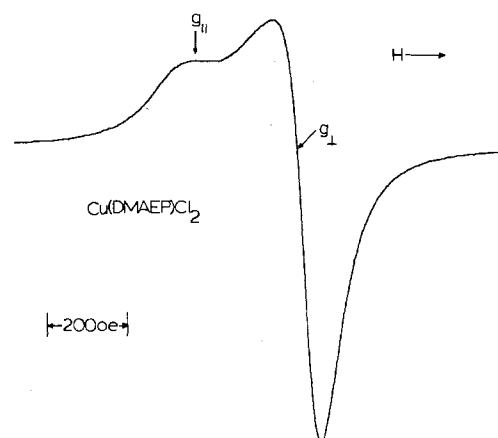
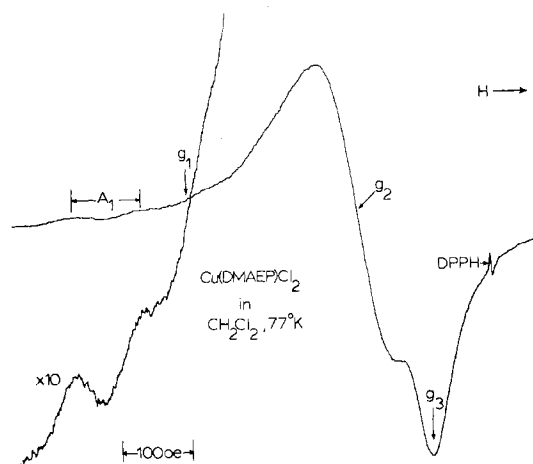
chelate bite of 95.34° in Cu(DMAEP)Cl₂ is similar to those of 95.02 and 95.20° in α - and β -[Cu(DMAEP)OH]₂(ClO₄)₂, respectively, where the boat conformation is adopted. Thus, there is no obvious reason why the half-chair conformation is unique to Cu(DMAEP)Cl₂ when the aromatic character of the N(1)-C(2) bond makes it a viable conformation in all AEP complexes.

Distortions from idealized bond angles are to be expected in chelate complexes, where the relative inflexibility of the chelate "bite" may not permit the angle subtended by the chelate at the metal to reach the value found in the regular figure. Hence, in the approximately tetrahedral complex³⁵ Zn(phen)Cl₂ the N-Zn-N angle is only 80.4° because the phenanthroline "bite" is only 2.67 Å. More significant, however, are the dihedral angles containing the metal, e.g., the angle between the planes Cu, L₁, L₂ and Cu, L₃, L₄, which would be 0 and 90° in the square planar (neglecting planes formed by trans ligands) and tetrahedral geometries, respectively. In Zn(phen)Cl₂, for example, the plane Zn, Cl(1), Cl(2) is inclined at an angle of 79.0° to the plane through the chelate; this value is clearly much closer to the tetrahedral value (90°) than to the square-planar value (0°). In the present complex, these dihedral angles are in the range 39-62°, intermediate between the two idealized forms. Hence, the distortions here are similar to (although greater than) those found³⁶ in the (-)- β -isosparteine complex of CuCl₂, which shows a range³⁷ of 47-81°.

Electronic Spectra. Electronic spectral data are summarized in Table VI. Both Cu(DMAEP)Cl₂ and its isomorphous bromide analogue exhibit spectra having a broad band centered roughly at 950 nm with well-defined features at about 820 and 1040 nm. The absorption in this region can be assigned to "d-d" transitions, the intensities of the bands being derived from metal centered "d-p" mixing expected for noncentrosymmetric complexes and covalency effects.^{38,39} Crystal field and molecular orbital calculations for pseudotetrahedral CuL₂X₂ complexes with C_{2v} microsymmetry^{40,41} yield the energy level sequence: $d_{xz} \gg d_{x^2-y^2} > d_{yz} > d_{z^2} > d_{xy}$. Since the $d_{x^2-y^2}$ and d_{z^2} orbitals both belong to the a₁ irreducible representation of the C_{2v} point group, the levels are mixed and the indicated energy level sequence denotes the dominant d-orbital parentage of the states.^{40,41} The bands at about 820 nm are accordingly assigned to $d_{xz} \leftarrow d_{xy}$ promotions and those at about 1040 nm to $d_{xz} \leftarrow d_{yz}$ transitions with the remaining transitions contributing to the overall band envelopes. Data for pseudotetrahedral 2,2'-biquinoline complexes are included in Table VI for comparison. Except for somewhat more resolved structure in the bands of the 2,2'-biquinoline com-

Table VII. Electron Paramagnetic Resonance Data

Compound	Lattice	g_{\parallel}	g_{\perp}	$\langle g \rangle$	$\times 10^4 \text{ cm}^{-1}$		
					$\langle A \rangle$	A_{\parallel}	A_{\perp}
Cu(DMAEP)Cl ₂	Powder	2.259	2.022	2.101			
	CH ₂ Cl ₂ , RT			2.138	61.4		
Cu(DMAEP)Br ₂	CH ₂ Cl ₂ , 77 K	2.305	2.118, 2.057	2.160		97.5	
	Powder			2.125		$\Delta H_{pp} = 709 \text{ Oe}$	
	CH ₂ Cl ₂ , RT			2.132	65.3		
	CH ₂ Cl ₂ , 77 K	2.371	2.116	2.201	35	59.4	19.6

Figure 3. Room temperature X-band EPR spectrum of polycrystalline Cu(DMAEP)Cl₂.Figure 4. Frozen solution (77 K) X-band EPR spectrum of Cu(DMAEP)Cl₂ in dichloromethane.

plexes, the two sets of compounds exhibit reasonably comparable spectra which are related to those reported for various tetrahalocuprate(II) distortion isomers.⁴²

The mull (transmission) spectra of Cu(DMAEP)Cl₂ and Cu(DMAEP)Br₂ exhibit pronounced shoulders in the ultraviolet region. These shoulders can be assigned to ligand-to-metal charge-transfer transition of the π halogen \rightarrow 3d type.⁴³⁻⁴⁵ Charge-transfer transitions from the nitrogen donor sites of DMAEP are expected⁴⁶ to occur below 300 nm. In general, $\pi L \rightarrow 3d$ charge-transfer transitions of pseudotetrahedral CuL₂X₂ species are expected to follow the sequence $N > Cl > Br$.

Electron Paramagnetic Resonance Spectra. EPR spectral parameters are summarized in Table VII. The room temperature EPR spectrum of a polycrystalline sample of Cu(DMAEP)Cl₂ is shown in Figure 3. This typical "tetragonal" type EPR spectrum contrasts notably with the very broad single line ($\Delta_{\text{peak-to-peak}} = 709 \text{ Oe}$) EPR spectrum exhibited by isomorphous Cu(DMAEP)Br₂. Presumably, dipolar broadening and enhanced spin-lattice relaxation⁴⁷ of the bromide

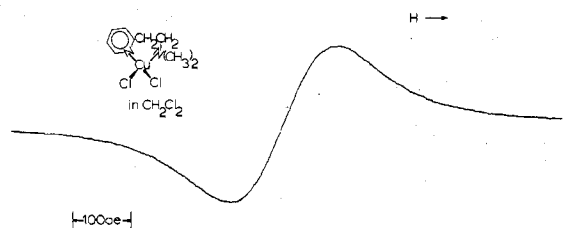


Figure 5. Room temperature EPR spectrum of $\text{Cu}(\text{DMAEP})\text{Cl}_2$ in dichloromethane.

complex account for the breadth and shape of the EPR spectrum. Magnetic dilution is achieved by dissolving the complexes in dichloromethane. The improved resolution of the g and hyperfine anisotropy of $\text{Cu}(\text{DMAEP})\text{Cl}_2$ in frozen dichloromethane solution is apparent in Figure 4. Unlike $\text{Cu}(\text{phen})\text{Cl}_2$ doped⁴⁸ into $\text{Zn}(1,10\text{-phen})\text{Cl}_2$,³⁶ no nitrogen superhyperfine splitting is resolved in frozen solutions containing $\text{Cu}(\text{DMAEP})\text{Cl}_2$ or $\text{Cu}(\text{DMAEP})\text{Br}_2$. For the latter complex only two of the three expected g values are resolved. An extensive analysis of the g and A values for pseudotetrahedral CuL_2X_2 species⁴¹ shows that (a) the largest g value is g_z , and that (b) the g_x, g_y, g_z g anisotropy is a complex function of an appreciable number of molecular orbital coefficients and the electronic transition energies. Hence, comments about the delocalization and bonding in complexes of this general type on the basis of limited EPR and electronic spectral data are somewhat restricted.⁴¹ The room temperature solution spectra of the DMAEP complexes are rather novel in that only single-line spectra (Figure 5) instead of the conventional four-line solution spectra are observed. The isotropic nuclear hyperfine coupling constants were estimated by taking one-third of the peak-to-peak width.^{40,41} EPR line widths of 10 Oe or more are not uncommon for copper(II) complexes, especially those not containing sulfur donor ligands, and when the hyperfine coupling is on the order of 60 Oe or less, a single EPR line for a solution spectrum becomes very probable.^{40,41} Similar spectra have been found for pseudotetrahedral $\text{Cu}(1\text{-sparteine})\text{X}_2$ ($\text{X} = \text{Cl}, \text{Br}$) and $\text{Cu}(2,2'\text{-biquinoline})\text{X}_2$ ⁴¹ compounds as well as the Schiff base complex bis(*N*-tert-butylpyrrole-2-carboxaldimino)copper(II).⁴⁹

The small values of the anisotropic hyperfine coupling constants and the single-line solution spectra found for the $\text{Cu}(\text{DMAEP})\text{X}_2$ species exhibit some similarities with comparable data for the "blue" copper proteins.⁵⁰ The "blue" copper proteins are, in part, characterized by small values of the parallel electron spin-nuclear spin hyperfine coupling constants ($A_{11} \lesssim 100 \times 10^{-4} \text{ cm}^{-1}$). An inspection of the published EPR spectra of "blue" proteins (see sources listed in ref 50) shows that the isotropic hyperfine coupling constants lie in the range $\sim 20\text{--}40 \times 10^{-4} \text{ cm}^{-1}$. This means that, if the "blue" copper proteins could tumble rapidly in solution, only single-line EPR spectra could be obtained. Although we do not envisage the DMAEP complexes discussed here as models for the "blue" copper proteins (largely because the characteristic intense electronic absorption band at about 600 nm is absent), it is worth noting that a number of authors have suggested⁵⁰⁻⁵³ a pseudotetrahedral geometry for the copper site in the "blue" proteins.

The origin of the small hyperfine coupling constants in pseudotetrahedral copper(II) complexes is associated with metal 4s and 4p orbital admixture into the ground state. In low-symmetry complexes 4s orbital participation in the ground state can be direct or easily "mixed in". The admixture of 4s orbital character into the ground state in noncentrosymmetric compounds provides a positive contribution⁵⁴ to the hyperfine splitting. Since the nuclear hyperfine couplings in centrosymmetric copper(II) complexes, which arise from core

polarization, have a negative sign, 4s orbital participation in the ground state brings about a reduction in the observed hyperfine coupling. Metal 4p orbital participation in the ground state can also contribute to a reduction in hyperfine coupling.^{41,55} In complexes such as $\text{Cu}(\text{DMAEP})\text{Cl}_2$ the metal 4p orbital may be estimated to participate in the ground state to the extent of about 4%.^{41,55} Analysis⁴¹ shows that 4s and 4p admixture into the ground state can lead to the loss of observable hyperfine splitting for pseudotetrahedral CuL_2X_2 species. (Quantitatively sorting out the various effects is decidedly nontrivial.) Yokoi^{53,56} has commented on this problem and has pointed out the need for additional calculations of spin-polarization of all of the metal s electrons associated with the exchange interaction with metal 4p orbital mixed into the ground state.

In summary, the structure of $\text{Cu}(\text{DMAEP})\text{Cl}_2$ has been found to consist of isolated pseudotetrahedral CuN_2Cl_2 chromophores. The intensities of the electronic absorption bands of $\text{Cu}(\text{DMAEP})\text{Cl}_2$ and its isomorphous bromine analogue and their EPR spectral properties are in accord with their pseudotetrahedral geometries. The present work provides significant additional support for spectra-structure correlations proposed for low-symmetry copper(II) compounds on the basis of rather meager evidence.

Registry No. $\text{Cu}(\text{DMAEP})\text{Cl}_2$, 64683-18-7; $\text{Cu}(\text{DMAEP})\text{Br}_2$, 64743-13-1.

Supplementary Material Available: A listing of structure factor amplitudes (12 pages). Ordering information is given on any current masthead page.

References and Notes

- E. Uhlig and M. Maaser, *Z. Anorg. Allg. Chem.*, **322**, 25 (1963).
- V. C. Copeland, W. E. Hatfield, and D. J. Hodgson, *Inorg. Chem.*, **12**, 1340 (1973).
- V. C. Copeland, W. E. Hatfield, and D. J. Hodgson, *Inorg. Chem.*, **11**, 1826 (1972).
- D. Y. Jeter, W. E. Hatfield, and D. J. Hodgson, *J. Phys. Chem.*, **76**, 2707 (1972).
- J. D. Dunitz, *Acta Crystallogr.*, **10**, 307 (1957).
- V. Kupcik and S. Durovic, *Czech. J. Phys.*, **10**, 182 (1960).
- B. Morosin, *Acta Crystallogr., Sect. B*, **31**, 632 (1975).
- V. F. Duckworth and N. C. Stephenson, *Acta Crystallogr., Sect. B*, **25**, 1795 (1969).
- P. Singh, D. Y. Jeter, W. E. Hatfield, and D. J. Hodgson, *Inorg. Chem.*, **11**, 1657 (1972).
- R. A. Bream, E. D. Estes, and D. J. Hodgson, *Inorg. Chem.*, **14**, 1672 (1975).
- R. B. Wilson, W. E. Hatfield, and D. J. Hodgson, *Inorg. Chem.*, **15**, 1712 (1976).
- D. H. Svedung, *Acta Chem. Scand.*, **23**, 2865 (1969).
- E. D. Estes, W. E. Hatfield, and D. J. Hodgson, *Inorg. Chem.*, **14**, 106 (1975).
- W. Stahlin and H. R. Oswald, *Acta Crystallogr., Sect. B*, **27**, 1368 (1971).
- E. D. Estes and D. J. Hodgson, *J. Chem. Soc., Dalton Trans.*, 1168 (1975).
- F. Hanic, *Acta Crystallogr.*, **12**, 739 (1959).
- M. Laing and E. Horsfield, *Chem. Commun.*, 735 (1968).
- M. Laing and G. Carr, *J. Chem. Soc. A*, 1141 (1971).
- P. W. R. Corfield, R. J. Doedens, and J. A. Ibers, *Inorg. Chem.*, **6**, 197 (1967).
- W. R. Busing and H. A. Levy, *J. Chem. Phys.*, **26**, 563 (1967).
- S. A. Goldfield and K. N. Raymond, *Inorg. Chem.*, **10**, 2604 (1971).
- J. R. Wasson, *Chemist-Analyst*, **56**, 36 (1967).
- I. Bernal and P. H. Riger, *Inorg. Chem.*, **2**, 256 (1963); D. H. Chen and G. R. Luckhurst, *Trans. Faraday Soc.*, **65**, 656 (1969).
- J. A. Ibers and W. C. Hamilton, Ed., "International Tables for X-Ray Crystallography", Vol. IV, Kynoch Press, Birmingham, England, 1974, (a) Table 2.2A, (b) Table 2.3.1.
- R. F. Stewart, E. R. Davidson, and W. T. Simpson, *J. Chem. Phys.*, **42**, 3175 (1965).
- Supplementary material.
- P. Singh, V. C. Copeland, W. E. Hatfield, and D. J. Hodgson, *J. Phys. Chem.*, **76**, 2887 (1972).
- V. C. Copeland and D. J. Hodgson, *Inorg. Chem.*, **12**, 2157 (1973).
- D. L. Kozlowski and D. J. Hodgson, *J. Chem. Soc., Dalton Trans.*, 55 (1975).
- D. L. Lewis and D. J. Hodgson, *Inorg. Chem.*, **13**, 143 (1974).
- D. L. Lewis and D. J. Hodgson, *Inorg. Chem.*, **12**, 2935 (1973).
- D. L. Lewis, W. E. Hatfield, and D. J. Hodgson, *Inorg. Chem.*, **11**, 2216 (1972).
- D. L. Lewis, W. E. Hatfield, and D. J. Hodgson, *Inorg. Chem.*, **13**, 147 (1974).

- (34) D. L. Lewis, K. T. McGregor, W. E. Hatfield, and D. J. Hodgson, *Inorg. Chem.*, **13**, 1013 (1974).
- (35) C. W. Reimann, S. Block, and A. Perloff, *Inorg. Chem.*, **5**, 1185 (1966).
- (36) L. S. Childers, K. Foltling, L. L. Merritt, Jr., and W. E. Streib, *Acta Crystallogr., Sect. B*, **31**, 924 (1975).
- (37) Calculated from the data in ref 36.
- (38) D. K. Johnson, H. J. Stoklosa, J. R. Wasson, and H. E. Montgomery, *J. Inorg. Nucl. Chem.*, **36**, 525 (1974).
- (39) J. R. Wasson, H. W. Richardson, and W. E. Hatfield, *Z. Naturforsch. B*, **32**, 551 (1977).
- (40) S. N. Choi, R. D. Bereman, and J. R. Wasson, *J. Inorg. Nucl. Chem.*, **37**, 2087 (1975).
- (41) J. R. Wasson, D. M. Klassen, H. W. Richardson, J. W. Hall, and W. E. Hatfield, submitted for publication.
- (42) D. W. Smith, *Coord. Chem. Rev.*, **21**, 93 (1976).
- (43) A. B. P. Lever, *J. Chem. Educ.*, **51**, 612 (1974).
- (44) B. D. Bird and P. Day, *J. Chem. Phys.*, **49**, 392 (1968); J. C. Rivoal and B. Briat, *Mol. Phys.*, **27**, 1081 (1974).
- (45) J. Demuyneck, A. Veillard, and U. Wahlgren, *J. Am. Chem. Soc.*, **95**, 5563 (1973).
- (46) E. W. Wilson, Jr., M. H. Kasperian, and R. B. Martin, *J. Am. Chem. Soc.*, **92**, 5365 (1970).
- (47) R. A. Vaughan, *Phys. Status Solidi B*, **49**, 274 (1972).
- (48) G. F. Kokoszka, C. W. Reimann, and H. C. Allen, *J. Phys. Chem.*, **71**, 121 (1967).
- (49) J. R. Wasson, *Spectrosc. Lett.*, **9**, 95 (1976).
- (50) J. A. Fee, *Struct. Bonding (Berlin)*, **23**, 1 (1975).
- (51) E. I. Solomon, J. W. Hare, and H. B. Gray, *Proc. Natl. Acad. Sci. U.S.A.*, **73**, 1389 (1976).
- (52) O. Siiman, N. M. Young, and P. R. Carey, *J. Am. Chem. Soc.*, **98**, 744 (1976).
- (53) H. Yokoi and A. W. Addison, *Inorg. Chem.*, **16**, 1341 (1977); U. Sakaguchi and A. W. Addison, *J. Am. Chem. Soc.*, **99**, 5189 (1977).
- (54) A. J. Freeman and R. E. Watson, "Magnetism", Vol. IIA, G. T. Rado and H. Suhl, Ed., Academic Press, New York, N.Y., 1965, p 67.
- (55) M. Sharnoff, *J. Chem. Phys.*, **42**, 3383 (1963); C. A. Bates, W. S. Moore, K. J. Standley and K. W. H. Stevens, *Proc. Phys. Soc., London*, **79**, 73 (1963).
- (56) H. Yokoi, *Bull. Chem. Soc. Jpn.*, **47**, 3037 (1974).

Contribution from the Chemistry Division, Argonne National Laboratory, Argonne, Illinois 60439, and the Departments of Chemistry and Physics, Laboratory for Research on the Structure of Matter, University of Pennsylvania, Philadelphia, Pennsylvania 19174

A Neutron Diffraction Investigation of the Crystal and Molecular Structure of the Anisotropic Superconductor Hg_3AsF_6

ARTHUR J. SCHULTZ,^{1a} JACK M. WILLIAMS,^{*1a} NEMESIO D. MIRO,^{1b} ALAN G. MACDIARMID,^{*1b} and ALAN J. HEEGER^{*1c}

Received July 7, 1977

The crystal and molecular structure of Hg_3AsF_6 has been investigated by single-crystal neutron diffraction. This metallic compound crystallizes in the body-centered tetragonal space group $I4_1/amd$ with cell dimensions of $a = 7.549$ (5) Å and $c = 12.390$ (9) Å. The crystal structure consists of two orthogonal and nonintersecting linear chains of $\text{Hg}^{0.33+}$ cations passing through a lattice of octahedral AsF_6^- anions. The intrachain Hg–Hg distance of 2.64 (2) Å is derived from planes of diffuse scattering normal to a^* and b^* . Since the a and b axis lattice constants are not simple multiples of the Hg–Hg intrachain distance, the mercury chains are incommensurate with the tetragonal lattice; hence we have the apparent formula $\text{Hg}_{2.86}\text{AsF}_6$. These results are in essential agreement with a previously reported x-ray diffraction study. However, from the neutron diffraction data, we have established that the Hg chains are *not* strictly one-dimensional. The maximum room-temperature deviation from the chain axis is 0.07 (1) Å with neighboring chains distorted away from each other. The closest interchain Hg–Hg contact is 3.24 (2) Å. Furthermore, analytical data consistently indicate a stoichiometric empirical formula of Hg_3AsF_6 . These results together with precise density measurements imply that the incommensurate structure is stabilized by anion vacancies, such that there are four formula weights of $\text{Hg}_{2.86}(\text{AsF}_6)_{0.953}$ per unit cell.

Introduction

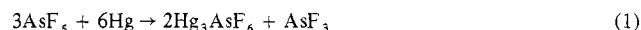
The properties of "low-dimensional" metals have been actively studied recently. Gillespie and co-workers² have reported the synthesis, structure, and properties of a novel $\text{Hg}_{2.86}\text{AsF}_6$ compound, containing two orthogonal and nonintersecting linear chains of mercury atoms. From the x-ray study,^{2a} diffuse planes of scattering intensity were observed normal to each chain direction, from which a Hg–Hg repeat distance of 2.64 (1) Å was obtained. The existence of the diffuse scattering indicated that the positions of the Hg atoms between neighboring chains are not correlated. Furthermore, the 2.64 Å repeat distance is incommensurate with the lattice dimensions ($a = b = 7.54$ Å) such that the nonstoichiometric empirical formula $\text{Hg}_{2.86}\text{AsF}_6$ was derived from the relationship $7.54/2.64 = 2.86$.

In order to investigate the physical properties of this material, we have developed procedures for the growth of large single crystals. The product analyzes as Hg_3AsF_6 , as also reported by Brown et al.^{2a} for what was reformulated as $\text{Hg}_{2.86}\text{AsF}_6$ based on the x-ray study. To verify the unusual structural model and provide additional structural data we undertook a neutron diffraction study, for which the problem of the dominance of Hg scattering is greatly lessened, as are the effects of absorption. We include, in addition, a summary of analytical data and the results of precise density measurements which have led us to conclude that this mercury chain salt is a stoichiometric compound in an incommensurate

structure stabilized by anion vacancies.

Experimental Section

Synthesis. The detailed procedures for the synthesis of large, silvery-golden crystals (up to $35 \times 35 \times 2$ mm) of Hg_3AsF_6 will be reported elsewhere.³ They involve the reaction of a solution of AsF_5 in liquid SO_2 with a mercury surface confined in 2-mm i.d. capillary tubing. To summarize, crystals are prepared by reacting either AsF_5^{2a} or $\text{Hg}_3(\text{AsF}_6)_2^{2c}$ with mercury in liquid SO_2 according to eq 1 and



2, respectively. Elemental analyses of the compound (Table I) show that it has the stoichiometric composition Hg_3AsF_6 .

In certain experiments large, silvery-golden crystals of apparent composition $\text{Hg}_3\text{AsF}_6\text{AsF}_3$ (Table I) were formed instead of the usual Hg_3AsF_6 . The exact conditions needed for the synthesis of $\text{Hg}_3\text{AsF}_6\text{AsF}_3$ are not clear and are presently under investigation. It appears that the formation may be initially dependent on the concentration of AsF_3 in the solution at the reaction site.

Neutron Diffraction Data Collection. A crystal of Hg_3AsF_6 was mounted under argon in a sealed lead-glass capillary in a general orientation, and all data were collected using an Electronics-and-Alloys four-circle goniostat at the Argonne CP-5 reactor in a manner previously described.⁴ The cell dimensions (see Table II) in the body-centered tetragonal space group $I4_1/amd$ (D_{4h}^{19} , No. 141)^{5a} were obtained from a least-squares fit of the angles 2θ , χ , and ϕ of 18 strong reflections ranging in 2θ from 41 to 54° (λ 1.142 (1) Å). Four forms of intensity data were measured for each crystal out to $(\sin \theta)/\lambda =$